

Effect of Physical Aging on Phenolphthalein Polyethersulfone/Poly(phenylene sulfide) Blend. I. Mechanical Properties

YUMING YANG,¹ ALBERTO D'AMORE,^{2,*} YINGWEI DI,¹ LUIGI NICOLAIS,² and BINYAO LI¹

¹Changchun Institute of Applied Chemistry, Chinese Academy of Sciences, Changchun 130022, People's Republic of China; ²Department of Materials and Production Engineering, University of Naples, Piazzale Tecchio, 80125 Naples, Italy

SYNOPSIS

The effect of physical aging at 210°C on the mechanical properties of phenolphthalein polyether sulfone (PES-C) and a PES-C/poly(phenylene sulfide) (PPS) blend, with 5% content of PPS, were studied using DMA, tensile experiments, an instrumented impact tester, and SEM observations. The blend shows good mechanical properties in comparison with the corresponding PES-C. The mechanical properties of both materials exhibit characteristics of physical aging, with only the aging rate of the blend relatively slower, which should be attributed to the constraint effect of PPS particles and the good interfacial adhesion. The morphology of the PPS phase in the blend did not change with aging time. The principal role of PPS particles is to induce crazes, which dissipate energy, under applied loading; thus, the blend shows good toughness. On the other hand, the multiple crazing mechanism depends on the molecular mobility or structural state of the matrix. © 1996 John Wiley & Sons, Inc.

INTRODUCTION

Glassy polymers are known to change their physical properties with time when used or stored at temperatures close to but below their glass transition temperature. The gradual molecular relaxation toward the thermodynamic equilibrium structure is commonly referred to as structure relaxation or, generally, as physical aging, which was summarized by Struik¹ and extensively studied by other researchers.¹⁻¹⁸ Due to the time dependence of the structure relaxation rate, physical aging is therefore a self-delaying phenomenon. The macroscopic properties of the polymer, during the aging process, will change with time. In general, with increasing aging time, the tensile strength, the density, and the excess enthalpy loss of polymers increase, while fracture energy or toughness and the physical aging rate decrease.

Blending of polymers has now become an established method of producing thermoplastic materials with an unusual combination of desirable properties. In recent years, for phenolphthalein polyethersulfone (PES-C), which is a novel high-performance thermoplastic with excellent mechanical strength and thermal resistance (T_g is about 245°C) developed in Changchun Institute under a Chinese patent,¹⁹ works have been done on blending it with a thermotropic liquid crystalline polymer (LCP)^{20,21} and poly(phenylene sulfide) (PPS)²² to improve its impact resistance and fracture toughness as well as processability. The incorporation of a small content of LCP or PPS into the PES-C matrix resulted in a significant increase in impact strength and fracture toughness and a reduction in flow viscosity without sacrificing the high mechanical strength and thermal resistance. While being used at high temperature, these blends will undergo a physical aging process, just like glassy polymers, during which the two phases may probably exhibit their own characteristics of aging and the microstructure of the blend may also change with time. A study of the physical

* To whom correspondence should be addressed.

aging effect on mechanical properties of these blends would yield valuable information.

Although enthalpy relaxation, representing the structure relaxation by a thermal method, in polymer blends, has become of increasing interest and has been reviewed by Mijovic et al.² and ten Brink et al.,³ only limited information exists about mechanical properties on the aging of polymer blends, especially for amorphous polymer-based blends. Mijovic et al.⁴ studied the effect of physical aging on stress relaxation in PMMA/SAN blends. Zhou and Hay²³ studied the structure–property relationships in annealed LLDPE/PP blends. Varin and Djokovic²⁴ reported the effect of annealing on PP/HDPE blends at 130°C. They considered that the annealing treatment improved the bonding between the phase-separated domains.

The present article investigates the effect of aging on the mechanical properties of PES-C/PPS blend with 5% content of PPS. The aim of this work was to determine if the blend can keep its good properties, in comparison with PES-C, after long-time aging.

EXPERIMENTAL

Materials and Sample Preparation

The amorphous PES-C resin used in this study was supplied by Xuzhou Engineering Plastic Co., China. Its reduced viscosity in chloroform at 25°C is 0.37 dL/g. High molecular weight grade PPS resin was supplied by Zigong Chemical Reagent Factory, China. Powders of PES-C and PPS were first mechanically mixed with a PPS weight composition of 5% at room temperature. The neat PES-C and mixture were then extruded in a twin-screw extruder (Model SHJ-30, China) at a melt temperature about 340°C. Dumbbell-shaped tensile specimens (ASTM D638, type V) and rectangular bars with size of 4 × 6 × 55 mm, for DMA and impact testing, were injection-molded in an injection-molding machine (Model JSW-17SA, Japan) with barrel temperatures of 325–350°C.

The physical aging of PES-C and the blend were carried out in an air-circulating oven at temperature 210°C up to 240 h. The original injection-molded specimens will be referred to as as-injection-molded specimens. After several months storage at room temperature, these specimens were tested. Because of very high T_g , there would be no further aging occurring in these specimens during storage at room temperature. This was confirmed by the differential

scanning calorimeter (DSC) results, which will be discussed in next report.

Mechanical Testing

Dynamic mechanical properties were determined at frequency of 1 Hz using a DuPont DMA983 instrument with a heating rate of 5°C/min. The heating program was set from 50 to 300°C.

An Instron 4204 testing machine was used to measure the tensile properties with a crosshead speed of 5 mm/min at room temperature. The unnotched Charpy impact tests were carried out in an instrumented impact tester (Model CEAST AFS/MK4) at room temperature.

Observation of Morphology

The fractured surface morphologies were observed using a scanning electron microscope (SEM) (Model S-2300, Hitachi). The samples were sputter-coated with gold before viewing under the microscope.

RESULTS AND DISCUSSION

Dynamic Mechanical Properties

The DMA provides us information about the structure changes of polymers taking place during the physical aging process. The storage modulus E' and loss tangent, $\tan \delta$, measured as a function of temperature, are shown in Figures 1 and 2 for PES-C and the PES-C/PPS blends, respectively. It can be seen that, for both materials with increasing aging

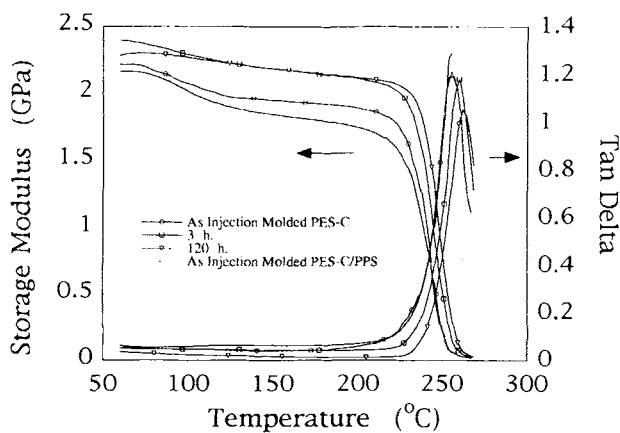


Figure 1 The storage modulus and $\tan \delta$ of PES-C as a function of temperature. For comparison, the curves for the as-injection-molded PES-C/PPS blend are also shown.

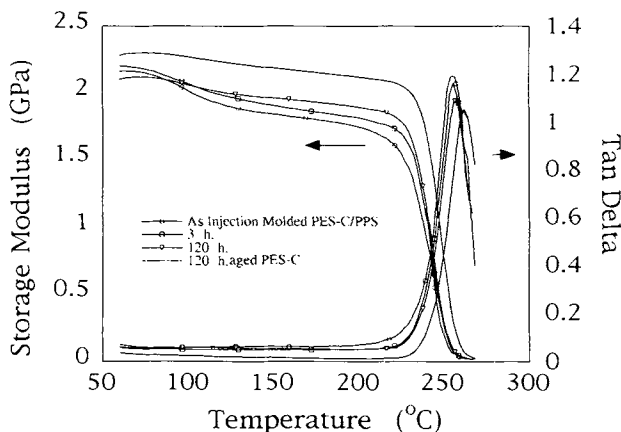


Figure 2 The storage modulus and $\tan \delta$ of the PES-C/PPS blend as a function of temperature. For comparison, the curves for 120 h aged PES-C are also shown.

time, E' increases while the $\tan \delta$ peak, which indicates the amount of energy dissipated as heat during the deformation of the material, shifts to higher temperature and the peak intensity decreases. Most of the changes of $\tan \delta$ appear at the lower-temperature side of each $\tan \delta$ peak for the temperature range investigated.

Previous work²² on the thermal and mechanical properties of PES-C/PPS blends showed that the blends were multiphase systems with small size and evenly dispersed PPS fibers and that strong interactions existed between the two phases. Within a PPS content of 25%, most of the PPS in the blends takes the amorphous form. For the aged PES-C/PPS blend, there seems to be no change in the morphology of the PPS phase.

In comparison with corresponding PES-C (i.e., for which with the same aging history), there is a small but obvious depression in storage modulus and a corresponding shoulder in $\tan \delta$ curves occurring at about 110°C, for as-injection-molded and aged blends, followed by a platform which holds up to the onset of glass transition temperature of the PES-C phase. One may attribute this T_g -type transition to the glass transition of the amorphous phase in PPS,

i.e., the amorphous phase of PPS in the blend can be well detected even though its content in the blend is only 5% and after long time aging. Together with the previous work,²² we may reach conclusions that most of the PPS in the blend takes the amorphous form and that physical aging, experienced at 210°C within the interesting period of time, has no or no obvious effect on the crystallinity of PPS. This is not surprising and is analogous to the result of Brady²⁵ who emphasized that annealing conducted below T_m had no or little effect on the crystallinity of PPS. Also, Cheung et al.²⁶ found that small particles of PPS in a polysulfone (PSF)/PPS (90/10) blend remained amorphous even after annealing at 160°C for 2 h. On the other hand, the morphology of the PPS phase in the blends depends on its compatibility with the matrix and/or processing conditions. By the method of NMR, Zhang and Wang²⁷ found that PPS/PES mechanically mixed blends were poorly compatible with a large domain size. But the solution-cast blends were partially compatible with a smaller domain size and lower crystallinity of PPS. As a result of partial compatibility between the PPS and PES-C matrix, the aging rate of PES-C in the blend should be affected by PPS particles due to the constraining effect.

The aging rates of PES-C and the PES-C/PPS blend are different as can be seen from Table I. Larger changes of the intensity and temperature of the $\tan \delta$ peak and E' (Fig. 1) have been found for PES-C after aging 120 h at 210°C, whereas these changes for the PES-C/PPS blend are relatively smaller. Therefore the aging rate, or the structure relaxation rate, of PES-C is faster than that of the PES-C/PPS blend. In other words, the relaxation of the PES-C matrix, at least those in the vicinity of PPS boundaries, was delayed by the PPS particles in the blend. This is more or less like the model for semicrystalline polymers proposed by Struik for the effect of the crystalline phase on the physical aging of semicrystalline polymers.⁵ The main feature of that model is that the crystals disturb the vicinal amorphous phase and reduce their segmental mo-

Table I The $\tan \delta$ Peak Temperature and Intensity of PES-C and the PES-C/PPS Blend

Aging Time Properties	0 h		3 h		120 h	
	Temp (°C)	Tan δ	Temp (°C)	Tan δ	Temp (°C)	Tan δ
PES-C	255.6	1.291	258.4	1.183	261.7	1.050
PES-C/PPS	253.6	1.214	255.2	1.164	256.8	1.093

bility. D'Amore et al.⁶ found that an increase of the amount of crystallite and fibers in the amorphous PEEK resulted in a slower sensitivity of the material to the volume relaxation. On the other hand, the physical aging rate, detected by enthalpy relaxation, was also found for some polymers to be reduced by incorporation of the second phase. The enthalpy relaxation rate in copolymers of styrene and butyl methacrylate was reduced by incorporation of carbon black for the existence of a special interaction between the filler and the copolymer.⁸ The reactive oligomer acetylene-terminated sulfone (ATS) restricted the aging process of PES-C remarkably for the forming of a semipenetrating network within the cured ATS network and PES-C. But the aging behavior of PES-C remained unaffected by addition of carbon black or short carbon fiber for the lack of interfacial adhesion in these composites.⁹ Also, the retardation of aging rate in filled polymers was found to depend on the specific nature of the filler—more specifically, the surface chemistry and available surface area of the filler.¹⁰ As a conclusion, the slower physical aging rate for polymer blends and composites should be contributed to the restraint effect of the second phase and the good interfacial adhesion, which happens to be the reason for mechanical property, especially the toughness, improvements for these blends and composites.

Tensile Properties

The mechanical properties of the aged samples of PES-C and the PES-C/PPS blend were markedly different from that of the as-injection-molded samples. During tensile testing, a small extent of the necking process, which represents higher energy absorption by the specimen, was observed only for the as-injection-molded samples. For all aged specimens, localized yielding or brittle fracture behavior were observed, as shown in Figure 3. The tensile strength of PES-C increases with increasing aging time. A marked increasing takes place within the first several hours and then the tensile strength leveled off on further aging without a yield point on the stress-strain curves, which is characteristic of brittle fracture. The same tendency for tensile strength changing with aging time, which shows the self-delaying characteristic of the aging process, was observed previously.¹¹⁻¹⁴ This phenomenon may be explained by the following statement^{15,16}: There is a distinction between the yield stress and crazing stress of a material; ductile failure is produced by extensive yielding while crazing leads to a brittle mode of fracture. Physical aging leads to an increase in the yield

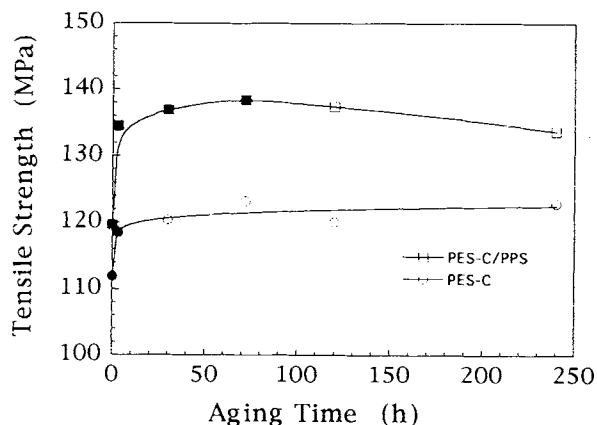


Figure 3 The tensile strength of PES-C and the PES-C/PPS blend as a function of aging time. Open circles represent brittle fracture stress and the filled circles denote yield strength.

strength but does not significantly change the fracture stress.

The same tendency for tensile strength changing with aging time can also be found for the PES-C/PPS blend within the first 100 h. But on further aging, a slight decrease of the tensile strength can be observed. A tentative explanation for this phenomenon is that when these PPS particles act as stress concentrators to initiate a multiplicity of crazes which can bear applied load further and the multiple crazing is the dominant deformation mechanism the blend may exhibit a macroscopic yielding process; thus, this yield strength may be a little higher than the brittle fracture stress. On the other hand, this multiple crazing mechanism, as discussed below, depends on the molecular mobility or structural state of the matrix. The structure relaxation of the matrix restrains this multiple crazing and makes the fracture in a brittle mode and thus results in the slight decrease of the tensile strength of the blend. It is obvious that the tensile strength of the blend is still higher than that of pure PES-C within the experimental time scale.

The fracture energy can be evaluated by the energy needed to break the specimen. Figure 4 shows the fracture energy for both materials as a function of aging time. As expected, the aged samples display a loss in their ductility. The blend shows always a higher fracture energy than that of pure PES-C. The fracture energy tendency to change with aging time for both materials is just the opposite to that of the tensile strength. Though the retardation of the physical aging rate in polymer blends and composites was found by DMA under a small strain condition, as discussed above, and mentioned by other

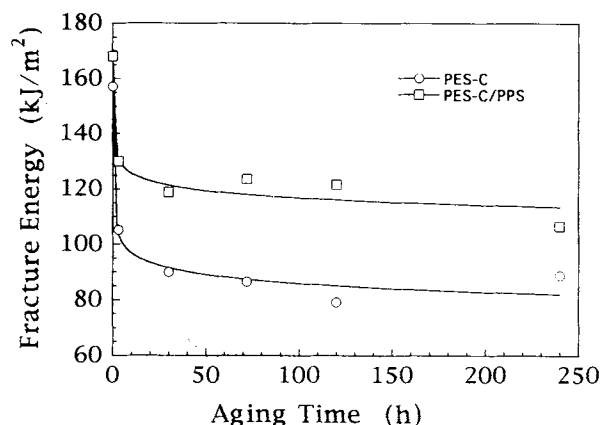


Figure 4 The tensile fracture energy of PES-C and the PES-C/PPS blend as a function of aging time.

researchers by means of volume relaxation⁶ or enthalpy relaxation,⁸⁻¹⁰ under a large deformation condition as for tensile testing, the aging rate for the PES-C/PPS blend seems to be similar to that of pure PES-C. As a whole, the blend shows good tensile properties even after long-time aging as compared with pure PES-C.

Impact Properties

The impact strength of the polymer is directly related to its toughness and defined as the ability of the material to absorb applied energy. The experimental data obtained from the instrumented impact tester showed that the impact fracture process of PES-C and the blend can be described as two steps: The first, up to F_{max} , which is the maximum force the material endured, representing the progressive energy absorption before microcrack initiation; the second, after the F_{max} , representing those microcracks' propagation to fracture. The unnotched Charpy impact fracture parameters are summarized in Table II. The $E_{(F_{max})}$ and E_t represent the energy absorption corresponding to the first step and total fracture process, which is the so-called impact strength.

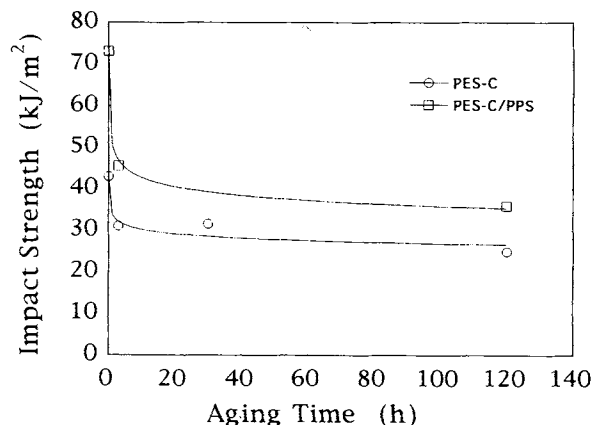


Figure 5 The impact strength of PES-C and the PES-C/PPS blend as a function of aging time.

As injection-molded and aged PES-C all exhibit brittle fracture behavior, and as a result of this, the $E_{(F_{max})}$ and E_t are almost the same. The F_{max} as well as $E_{(F_{max})}$ and E_t decrease with increasing aging time. On the other hand, these parameters for the blend are higher than that of pure PES-C. With increasing aging time, the $E_{(F_{max})}$ and E_t decrease in the same trend as that of pure PES-C, as shown in Figure 5, but the F_{max} does not change with time. This phenomenon should be attributed to the multiple crazing mechanism arising from those PPS particles. Therefore, the PES-C/PPS blend shows good impact properties even after long-time aging. For a better understanding of these mechanical properties, a study of fracture morphology is necessary.

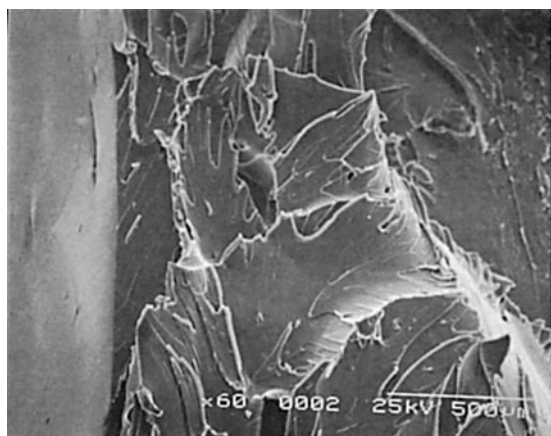
Morphological Studies

Morphological studies, with the aid of scanning electron microscopy (SEM), can help us trace back the source of the fracture and relate the mode of deformation to the microstructure of the material and the mechanical properties. At low magnification, we can observe the macroscopic fracture morphology. The impact fracture surface of the as-injection-molded PES-C/PPS blend gives clear evidence of

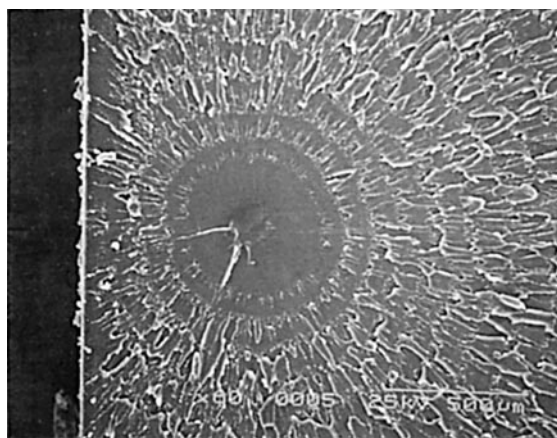
Table II Impact Properties of PES-C and the PES-C/PPS Blend

Aging Time Properties	0 h			3 h			120 h		
	F_{max} (N)	$E_{(F_{max})}$ (kJ/m ²)	E_t (kJ/m ²)	F_{max} (N)	$E_{(F_{max})}$ (kJ/m ²)	E_t (kJ/m ²)	F_{max} (N)	$E_{(F_{max})}$ (kJ/m ²)	E_t (kJ/m ²)
PES-C	348	42	43	322	29	31	301	25	25
PES-C/PPS	357	58	73	356	39	46	358	35	36

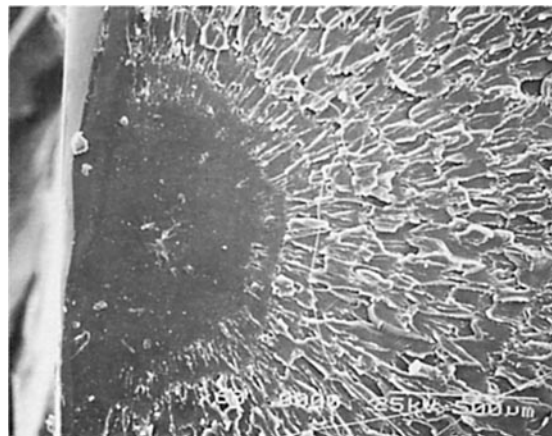
ductility on the fracture surface [Fig. 6(a)]. Close to the fracture initiation site, there exists evidence of bulk shrinkage and plastic deformation, generating randomly on different planes from several initiators. Coming next on the surface is the faster fracture region with flat surface showing a brittle fracture mode. Also, some macrocracks on different planes under the fractured surface were seen on the side face. On the other hand, the aged (120 h) specimen shows a typical brittle fracture mode, as shown in Figure 6(b). Close to its fracture initiation site is a smooth so-called mirror region representing the slow crack growth region. This is surrounded by a



(a)



(b)



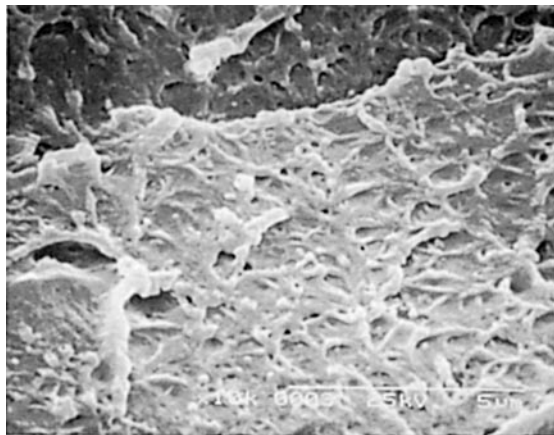
(c)

Figure 6 (Continued)

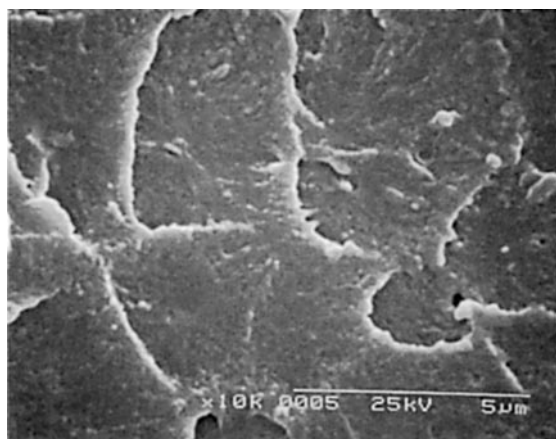
radiating and concentric band structure, the so-called patch pattern^{7,28} or hackle bands,²⁹ characteristic of a fast growth region. The as-injection-molded and aged PES-C show the same macroscopic fracture mode as that of the aged PES-C/PPS blend, as shown in Figure 6(c). This morphology has also been reported in many other kinds of materials such as PET¹⁷ and PEEK.¹⁸

At high magnification, the microstructure and microscopic deformation mode of the material can be observed. Previous works had attributed the toughness improvement of PES-C by blending LCP²¹ or PPS²² to the good interfacial adhesion. The present results show that the good interfacial adhesion did not change by physical aging. The view of a portion of the fracture surface near the initiation region, for the as-injection-molded PES-C/PPS blend indicates that considerable localized plastic deformation is present [Fig. 7(a)]. A round and smooth PPS fiber end can be found in each smaller localization. This morphology gives the impressions that craze initiation is preferably induced at or near PPS fiber ends and nearly every PPS fiber end can act as a stress concentrator to initiate craze. The morphology of the 120 h aged specimen is quite different; only some relatively large PPS fibers can be found in each localization from the fractured surface. But there is also no cavitation around these fibers. This implies that the good interfacial adhesion between PES-C and PPS did not change during the physical aging process. This is obvious because the microstructure of the rubbery state PPS phase did not change with aging time and those fine and evenly dispersed PPS fibers remain amorphous as discussed above. The physical aging, on a molecular level, is

Figure 6 SEM photographs of the impact-fractured surfaces of the (a) as-injection-molded PES-C/PPS blend, (b) 120 h aged blend, and (c) as-injection-molded PES-C.



(a)



(b)

Figure 7 SEM photographs (high magnification) of the impact-fractured surfaces of the (a) as-injection-molded PES-C/PPS blend and (b) 120 h aged blend.

thought to accompany the motion of the polymer chains into a tighter packing density, the volume relaxation, for amorphous polymers. As a result of this tighter packing, the original possible intervals might disappear. At least, the original interfacial adhesion did not change.

Based on these morphologies, it is suggested that the principal role of PPS fibers in the blend is to induce multiple crazing under an applied loading at their ends; thus, the blend shows more ductility than does pure PES-C. After a long aging time, however, there are not as many PPS fiber ends as in an as-injection-molded blend that can act as stress concentrators to initiate a multiplicity of small crazes.

This phenomenon should be attributed to the physical aging of the PES-C matrix. In fact, the ability to deform and absorb energy under an applied loading depends on the ease with which its molecular chains can slide past each other or change molecular conformations. This ability, as a result of the localized plastic deformation of the matrix occurring after the initiation of crazes, decreased markedly with increasing aging time, as shown by its mechanical properties above. Even if the PPS fiber ends can act as stress concentrators to initiate multiple crazing, the ease of these having generated craze growth, during which further crazes initiate depends primarily on the structural state of the matrix and how this state changes with time. Therefore, for a long-time-aged blend, crack propagation, based on the growth of crazes generated around relatively larger-size PPS fibers, may pass through all the other PPS fibers before further crazes initiate around them. So, the crack propagation energy was lower than that of the as-injection-molded specimen.

CONCLUSIONS

The effect of physical aging at 210°C on the mechanical properties of the PES-C/PPS (95/5) blend and pure PES-C have been studied. It was found that the blend always shows good mechanical properties as compared with pure PES-C. The tensile strength and impact strength for both materials change markedly with increasing aging time within the first several hours. On further aging, these properties leveled off gradually, thus exhibiting the self-delaying nature of physical aging. Only the aging rate of the blend is relatively slower.

On the microscopic level, the morphology of the PPS phase and the good interfacial adhesion between the two phases in the blend did not change with aging time. For this reason, the structure relaxation of the PES-C matrix was restrained by the finely dispersed PPS particles and, therefore, the blend shows a slower aging rate than that of pure PES-C. The principal role of PPS particles is to induce many small crazes under applied loading, thus dissipating energy and making the blend show good toughness. On the other hand, the multiple crazing mechanism depends on the molecular mobility or structural state of the matrix.

Y. Y. would like to thank A. Visconti, G. Arpaia, and G. Carotenuto for their assistance with the experiments. Part of this work was supported by the Chinese National Natural Science Foundation and Jilin Province Foundation.

The Chinese Academy of Sciences (China) and National Research Council (Italy) are gratefully acknowledged for financial support.

REFERENCES

1. L. C. E. Struik, *Physical Aging in Amorphous and other Materials*, Elsevier, Amsterdam, 1978.
2. J. Mijovic, L. Nicolais, A. D'Amore, and J. M. Kenny, *Polym. Eng. Sci.*, **34**, 381 (1994).
3. G. ten Brink, L. Oudhuis, and T. S. Ellis, *Thermochim. Acta*, **238**, 75 (1994).
4. J. Mijovic, S. T. Devine, and T. Ho, *J. Appl. Polym. Sci.*, **39**, 1133 (1990).
5. L. C. E. Struik, *Polymer*, **28**, 1521 (1987).
6. A. D'Amore, F. Cocchini, A. Pompo, A. Apicella, and L. Nicolais, *J. Appl. Polym. Sci.*, **39**, 1163 (1990).
7. A. J. Hill, K. J. Heater, and C. M. Agrawal, *J. Polym. Sci. Part B*, **28**, 387 (1990).
8. S. Kumar and R. Salovey, *J. Appl. Polym. Sci.*, **30**, 2315 (1985).
9. K. Mai, H. Zeng, and M. Zhang, *Acta Polym. Sin. (China)*, **1**, 53 (1993).
10. R. A. Shanks, *Br. Polym. J.*, **18**, 75 (1986).
11. J. A. Zurimendi, F. Biddlestone, J. N. Hay, and R. N. Haward, *J. Mater. Sci.*, **17**, 199 (1982).
12. T. -D. Chang and J. O. Brittain, *Polym. Eng. Sci.*, **22**, 1221 (1982).
13. J. R. Flick and S. E. B. Petrie, in *Structure and Properties of Amorphous Polymers*, A. G. Walton, Ed., Elsevier, Amsterdam, 1980.
14. Y. Yang, T. He, and F. Yu, *J. Appl. Polym. Sci.*, **55**, 627 (1995).
15. G. L. Pitman, I. M. Ward, and R. A. Duckett, *J. Mater. Sci.*, **13**, 2092 (1978).
16. I. M. Ward, *Mechanical Properties of Solid Polymers*, Wiley-Interscience, New York, 1971.
17. A. Aref-Azar, F. Biddlestone, J. N. Hay, and R. N. Haward, *Polymer*, **24**, 1245 (1983).
18. D. J. Kemmish and J. N. Hay, *Polymer*, **26**, 905 (1985).
19. K. Liu, H. Zhang, and T. Chen, Chin. Pat. 85101721.5 (1985).
20. G. Li, J. Yin, B. Li, G. Zhuang, and Y. Yang, *Polym. Eng.*, **35**, 658 (1995).
21. Y. Yang, J. Yin, B. Li, G. Zhuang, and G. Li, *J. Appl. Polym. Sci.*, **52**, 1365 (1994).
22. Y. Yang, B. Li, Y. Zhang, and G. Zhuang, *J. Appl. Polym. Sci.*, **55**, 633 (1995).
23. X. Zhou and J. N. Hay, *Polymer*, **34**, 4710 (1993).
24. R. A. Varin and D. Djokovic, *Polym. Eng. Sci.*, **28**, 1477 (1986).
25. D. G. Brady, *J. Appl. Polym. Sci.*, **20**, 2541 (1976).
26. M.-F. Cheung, A. Golovoy, H. K. Plummer, and H. van Oene, *Polymer*, **31**, 2299 (1990).
27. X. Zhang and Y. Wang, *Polymer*, **30**, 1867 (1989).
28. A. Siegmann and A. Hiltner, *Polym. Eng. Sci.*, **24**, 869 (1984).
29. M. A. Bellinger, J. A. Sauer, and M. Hara, *Polymer*, **35**, 5478 (1994).

Received April 12, 1995

Accepted August 16, 1995